

Influence of solvent granularity on the effective interaction between charged colloidal suspensions

E. Allahyarov and H. Löwen

Institut für Theoretische Physik II, Heinrich-Heine-Universität Düsseldorf, D-40225 Düsseldorf, Germany
(March 6, 2019)

We study the effect of solvent granularity on the effective force between two charged colloidal particles by computer simulations of the primitive model of strongly asymmetric electrolytes with an explicitly added hard sphere solvent. Apart from molecular oscillating forces for nearly touching colloids which arise from solvent and counterion layering, the counterions are attracted towards the colloidal surfaces by solvent depletion providing a simple statistical description of hydration. This, in turn, has an important influence on the effective forces for larger distances which are considerably reduced as compared to the prediction based on the primitive model. When these forces are repulsive, the long-distance behaviour can be described by an effective Yukawa pair potential with a solvent-renormalized charge. As a function of colloidal volume fraction and added salt concentration, this solvent-renormalized charge behaves qualitatively similar to that obtained via the Poisson-Boltzmann cell model but there are quantitative differences. For divalent counterions and nano-sized colloids, on the other hand, the hydration may lead to overscreened colloids with mutual attraction while the primitive model yields repulsive forces. All these new effects can be accounted for through a solvent-averaged primitive model (SPM) which is obtained from the full model by integrating out the solvent degrees of freedom. The SPM was used to access larger colloidal particles without simulating the solvent explicitly.

PACS: 82.70.Dd, 61.20.Ja

I. INTRODUCTION

Most of soft matter systems, as colloids, polymers or biological macromolecules, are dispersed in a molecular solvent [1]. Therefore, a full statistical description of supramolecular solutions should include the solvent explicitly. Such a treatment is highly non-trivial, however, since the length scale separation between the mesoscopic particles and the molecular solvent directly implies that the number of solvent particles which have to be included is enormous. On the other hand, one is interested mainly in properties of the big particles such that a solvent pre-average makes sense. The crudest form of such a course-grained level is to treat solvent properties just by a dielectric background or by some effective parameters which enter in the effective colloidal interactions. This procedure is questionable for polyelectrolytes where the solvent couples directly to the counterions which may affect the effective interaction between the polyelectrolytes via the long-ranged Coulomb coupling of counterions to the polyelectrolytes.

In this paper, we consider the case of two spherical charged colloidal particles (polyions) which are immersed in a bath of the molecular solvent and their oppositely charged counterions plus additional salt ions [2]. Our main focus is the total effective force acting onto the colloidal pair which is the key quantity to understand colloidal stability and which governs colloidal correlations and phase transitions. In almost any theoretical treatment, the discrete structure of the solvent particles was neglected and only the charged constituents were treated explicitly within the so-called “primitive” model (PM) of

strongly asymmetric electrolytes. Even this model is non-trivial in the colloidal context due to the large asymmetry between poly- and counterions and bears a rich physics resulting from the strong coupling between the different species. In recent computer simulations [3–7], counterionic correlations have been shown to be responsible for effective attractions between the like-charge polyions. The PM, re-formulated in terms of modern density functional theory of the inhomogeneous counterion plasma [8], can also be used as a starting point to derive simpler theories such as the mean-field nonlinear Poisson-Boltzmann approach or the linearized Debye-Hückel-type screening theory. The latter results in an effective Yukawa pair potential between the colloids as given by the electrostatic part of the celebrated Derjaguin-Landau-Verwey-Overbeek (DLVO) theory [9]. This potential can also be used with renormalized parameters to include parts of the nonlinear screening effects arising from Poisson-Boltzmann theory [10].

In the present paper, we investigate the influence of *solvent granularity* on the effective interactions between charged colloids. We model the solvent as a hard sphere fluid at intermediate packing fractions and use computer simulations and the theoretical concept of effective interactions to derive effects due to the discrete solvent. The PM is tested against this more general model. Although the hard sphere model neglects some important solvent properties as its polarizability [11] and its permanent multipole moments [12], it provides a minimal framework to get insight into counterion hydration and screening effects. The hard sphere solvent model (which is sometimes called solvent-primitive model) has been

used also in many other investigations of ordinary electrolytes and for electrolytes confined between two parallel charged plates. Most of the approaches invoke additional approximations as different versions of liquid-integral equations [13,12,14], Poisson-Boltzmann theory suitably modified to include the short-ranged solvent depletion effects [15], or more sophisticated density functional approaches of multicomponent systems [16]. For charged plates [17] and for small neutral particles [18] some computer simulations have already been performed including a hard sphere solvent explicitly but there are no results for charged colloidal spheres.

Most of the results in this paper are based on a new “solvent bath” simulation scheme which allows to simulate many neutral spheres together with the charged species. For divalent counterions, we obtain attractive forces due to overscreening of polyions by counterions which are attracted towards the colloidal surfaces via hydration (or solvent depletion) forces. For monovalent counterions and large distances we show that the concept of charge renormalization can be used to extract a Yukawa picture of the effective interaction with a solvent-renormalized polyion charge. We check the trends of this renormalized charge with respect to the colloidal density and the concentration of added salt and find qualitative agreement but quantitative differences as compared to the Poisson-Boltzmann theory. All our results can be reproduced within a solvent-averaged primitive model (SPM) which was extensively used in earlier theoretical studies of electrolytes between plates [13,19]. This idea originates from McMillan and Mayer [20] dating back to 1945.

Our paper is organized as follows: In chapter II, we describe our model and define approximations on different levels. The computer simulation method is described in chapter III. We then turn to results for the neutral case in chapter IV and for the salt-free case in chapter V. Parts of the latter have been published elsewhere [21]. The effect of added salt is described in chapter VI and other mechanisms of polyion-polyion attraction are critically discussed in chapter VII. We finally conclude in chapter VIII.

II. MODELING ON DIFFERENT LEVELS

In this section we summarize the modeling on different levels. In the following we shall use the most detailed description of the hard sphere solvent model and test the validity of the different inferior levels with respect to our data.

A. The hard sphere solvent model (HSSM)

The hard sphere solvent model (HSSM) involves spherical polyions with diameter σ_p and homogeneously

smear charge q_p together with their counterions of diameter σ_c and charge q_c in a bath of a neutral solvent ($q_s = 0$) with diameter σ_s . In the absence of salt, the pair potentials between the particles as a function of their mutual distances r are a combination of excluded volume and Coulomb terms

$$V_{ij}(r) = \begin{cases} \infty & \text{for } r \leq (\sigma_i + \sigma_j)/2 \\ q_i q_j / \epsilon r & \text{else} \end{cases} \quad (1)$$

where ϵ is the a smeared background dielectric constant of the solvent and $(ij) = (pp), (pc), (ps), (cc), (cs), (ss)$. Further parameters are the thermal energy $k_B T$ and the partial number densities ρ_i ($i = p, c, s$) which can be expressed as partial volume fractions $\phi_i = \pi \rho_i \sigma_i^3 / 6$ ($i = p, c, s$). Charge neutrality requires $\rho_p |q_p| = \rho_c |q_c|$. Additional salt ions can readily be included into the description as further charged hard spheres.

B. The solvent-averaged primitive model (SPM)

For a fixed configuration of charged particles the solvent can be traced out exactly arriving at depletion forces $\vec{F}_i^{(d)}$ acting onto the i th charged particle. They can be related to a surface integral over the solvent equilibrium density field $\rho_s(\vec{r})$ which depends parametrically on the positions of the fixed charged particles:

$$\vec{F}_i^{(d)} = k_B T \int_{S_i} d\vec{f} \rho_s(\vec{r}) \quad (2)$$

where \vec{f} is a surface vector pointing towards the center of the i th charged particle. If one adds these forces to the PM, the resulting model is strictly equivalent to the HSSM. The integrand $\rho_s(\vec{r})$ is affected by the space excluded for the solvent due to the presence of the finite core of the charged particles resulting in inhomogeneous density distributions around the excluded volume. The range of this inhomogeneity is characterized by the hard sphere bulk correlation length ξ which depends on the solvent packing fraction ϕ_s . A further approximation decomposes the forces $\vec{F}_i^{(d)}$ into pairwise parts, i.e. into a superposition of pair contributions coming from neighboring charged particles. This approximation is justified if the average distance between triplets, quadruplets, etc. of charged particles is much larger than the bulk correlation length ξ . In the salt-free case, this is generally granted except for nearly touching polyions with squeezed counterions. If salt is added, the justification is less clear as ion pairing by counter- and coions near polyions may be an important configuration.

The resulting pairwise interactions define the solvent-averaged model (SPM) where the depletion pair potentials $V_{ij}^{(d)}(r)$ ($(ij) = (pp), (pc), (cc)$) have to be added to the interactions of the primitive model of the next paragraph. These pairwise depletion forces have been the subject of intense recent research [22–27]. In particular,

we will determine them by computer simulation, and use these results as an input for the SPM.

C. The primitive model (PM)

The primitive model has the same interactions as the HSSM except for the absence of the solvent. Hence the basic interactions are again

$$V_{ij}(r) = \begin{cases} \infty & \text{for } r \leq (\sigma_i + \sigma_j)/2 \\ q_i q_j / \epsilon r & \text{else} \end{cases} \quad (3)$$

but now for $(ij) = (pp), (pc), (cc)$ only.

D. DLVO-theory

In DLVO theory, only the polyions are treated explicitly. The electrostatic part of their interaction is an effective Yukawa pair potential which has the form:

$$V(r) = \frac{q_p^2 \exp(-\kappa(r - \sigma_p))}{(1 + \kappa\sigma_p/2)^2 \epsilon r} \quad (4)$$

with

$$\kappa = \sqrt{4\pi\rho_c q_c^2 / \epsilon k_B T} \quad (5)$$

E. The PB-renormalized Yukawa model (PBYM)

This approach was suggested by Alexander et al [10] and is based on Poisson-Boltzmann theory in a spherical cell around a single polyion. The cell radius R is fixed by the polyion concentration:

$$R = (4\pi\rho_p/3)^{-1/3} \quad (6)$$

Within Poisson-Boltzmann theory, one calculates the counterion density $\tilde{\rho}_c$ at the cell boundary. Linearizing the nonlinear Poisson-Boltzmann theory at the cell boundary, one obtains again an effective Yukawa potential between the colloids arriving at the PB-renormalized Yukawa model (PBYM). The Yukawa potential has the same form as in Eqn.(4) but contains a renormalized inverse screening length

$$\kappa^* = \kappa \sqrt{\frac{\tilde{\rho}_c}{\rho_c}} \quad (7)$$

and a *renormalized charge*

$$q_p^* = q_p \frac{\tilde{\rho}_c}{\rho_c} \quad (8)$$

which is considerably smaller than the bare charge q_p . Many experimental data for the colloidal structural correlations [28], the long-time self-diffusion [29] or the freezing line [30] have been analyzed using this concept of charge renormalization and in general good agreement was found for monovalent counterions provided the colloids are far away from charged plates [31].

F. The solvent-renormalized Yukawa model (SYM)

This approach is a generalization of the Poisson-Boltzmann cell model [10] to the presence of a granular solvent. Again, one considers a single polyion in a spherical cell, but uses the full HSSM to obtain the counterion density $\tilde{\rho}_c$ at the cell boundary. As in the PBYM, the associated Yukawa pair potential has a solvent-renormalized inverse screening length κ^* and a solvent-renormalized charge q_p^* , which, however, differ from that of the PBYM approach.

III. SIMULATION METHOD

We consider two large spherical polyions in a cubic simulation box of length L with periodic boundary conditions, hence $\rho_p = 2/L^3$. The polyions are fixed along the body diagonal of the cubic box. While the simulation methods for the PM are straightforward and are described elsewhere [32,33], a significant volume fraction of solvent particles together with large colloidal particles implies a huge number of solvent spheres in the simulation box.

As the solvent interactions are short ranged and the solvent-averaged interactions are only of range ξ , one can reduce the number of solvent particles in the simulation box considerably using a “solvent-bath” method. This procedure is sketched in Figure 1 and works as follows: we define a spherocylindrical cell around the colloidal pair such that the minimal distance h from the colloidal surface to the spherocylindrical boundary is much larger than the hard sphere bulk correlation length ξ . The hard sphere solvent is only contained in this spherocylinder. As the cell volume is considerably smaller than the volume $1/L^3$ of the whole simulation box, the number of solvent particles for fixed given volume fraction ϕ_s is drastically reduced. No restriction is done for the counter- and salt-ions, which can move within the whole simulation cell.

Care has to be taken at the artificial cell boundary. We use the Molecular Dynamics (MD) method calculating the particle trajectories and performing statistical averages over some physical quantities. The hard sphere solvent is treated by the well-known hard sphere collision rules. Once a solvent particle is leaving the spherocylindrical cell it is randomly inserted at another place of the cell boundary with the same velocity. The position of its

random insertion has a randomly chosen distance from the spherocylindrical boundary up to $2\sigma_s$ which avoids unphysical solvent layering there.

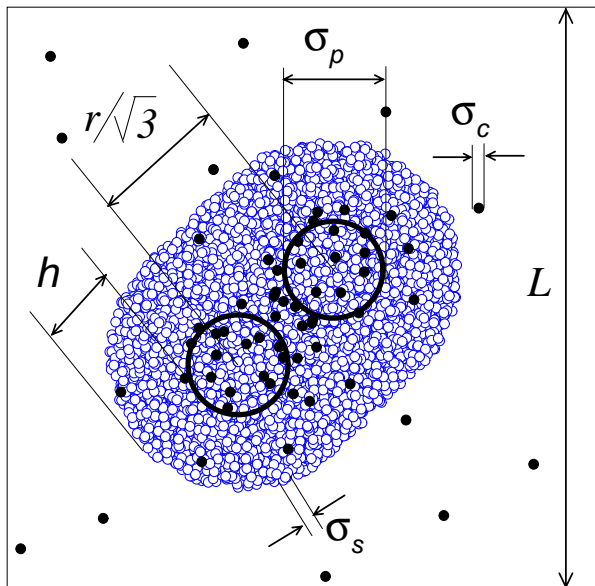


FIG. 1. View of the set-up as a downward projection of a simulation snapshot: Two polyions (dark open circles) in a bath of solvent particles (small hollow spheres) contained in a spherocylindrical cell of width h . The counterions shown as small dark spheres can move in the whole simulation box of size L . The distance between the polyions is r , hence the projected distance shown is $r/\sqrt{3}$.

Since the width of the cell h is much larger than the hard sphere bulk correlation length ξ , the presence of the boundary has no influence on the inhomogeneous density distribution of the solvent and the counterions near the colloidal surfaces. The counterion motion is implemented as follows: Outside the spherocylindrical cell the counterions interact via a solvent-averaged effective depletion potential. This is justified as the typical distance between the counterions is much larger than the hard sphere bulk correlation length ξ . Therefore, the correction to $V_{cc}(r)$ due to solvent layering is negligibly small anyway for counterions outside the spherocylindrical cell. This is not the case when salt is added as the attraction between co- and counterions may lead to short distances where solvent depletion effects may dominate the interactions. For a counterion approaching the cell boundary, there is an artificial asymmetry between the solvent bath inside the cell and the “vacuum” outside the cell which hinders a counterion to penetrate into the solvent bath. This unphysical effect is repaired in the simulation scheme by switching off the counterion-solvent interaction for a counterion which is penetrating from outside. Once the counterion is fully surrounded by solvent molecules the interaction is turned on again. This leads to a symmetric counterion crossing rate across the spherocylindrical cell boundary.

We have carefully tested the algorithm against simulations of small systems where the whole space was filled with solvent particles. We also tested against a situation of a solvent slab between charged plates. Perfect agreement was found compared to simulations where the whole space was filled with solvent particles.

IV. RESULTS FOR THE NEUTRAL CASE

Let us first discuss the much simpler case of neutral polyions ($q_p = 0$) under absence of counterions. The resulting system is just a pair of big hard spheres in a sea of small solvent spheres. This simple model for binary mixtures of hard sphere colloids has gained considerable attention during the past ten years. The effective interaction between the large spheres as induced by depletion of the small spheres in the zone intermediate between the nearly touching big spheres has the following characteristic features which were obtained by density functional theory [23–25], computer simulation [34,26,27] and experiments [35–37]: it is attractive for nearly touching spheres, then it oscillates with the bulk correlation length of the hard sphere solvent ξ . The depletion interactions decays to zero exponentially with the surface-to-surface separation of the big spheres. The characteristic decay length is again the bulk correlation length ξ .

Our motivation to investigate the neutral case is twofold: First, it is a simple case which allows to test our simulation set-up. There are some computer simulations of the depletion interaction in the literature but the range of parameters examined is far from being complete. Second, for the solvent-averaged primitive model (SPM) it is exactly the solvent depletion term (2) which one has to add to the primitive interactions as given by eqn.(3). Therefore, studies of the SPM require a full knowledge of the neutral case.

Computer simulation results for the total effective depletion force $F_{pp}^{(d)}(r)$ acting onto the big spheres are presented in Figure 2 for two size ratios σ_p/σ_s of 2 and 14. The solvent packing fraction was chosen to be $\phi_s = 0.3$. The force is projected onto the particle separation vector such that a positive sign means repulsion. We note that a direct evaluation of eqn. (2) is difficult as the solvent density field piles up strongly at the surfaces of the big particles. A much more effective way is to measure the momentum transfer on the fixed big spheres due to colliding small spheres during the Molecular Dynamics simulation. The results are compared with a recently proposed fitting formula of Roth and Evans based on density functional theory [38]. One sees that the contact value of the force and the oscillations are well-described by the theory but there are deviations around the first maximum. This is less apparent if the effective potential is compared as shown in the inset of Figure 2. Obviously, the reason for that is that the force is a derivative which is more sensitive to approximations. In the computer

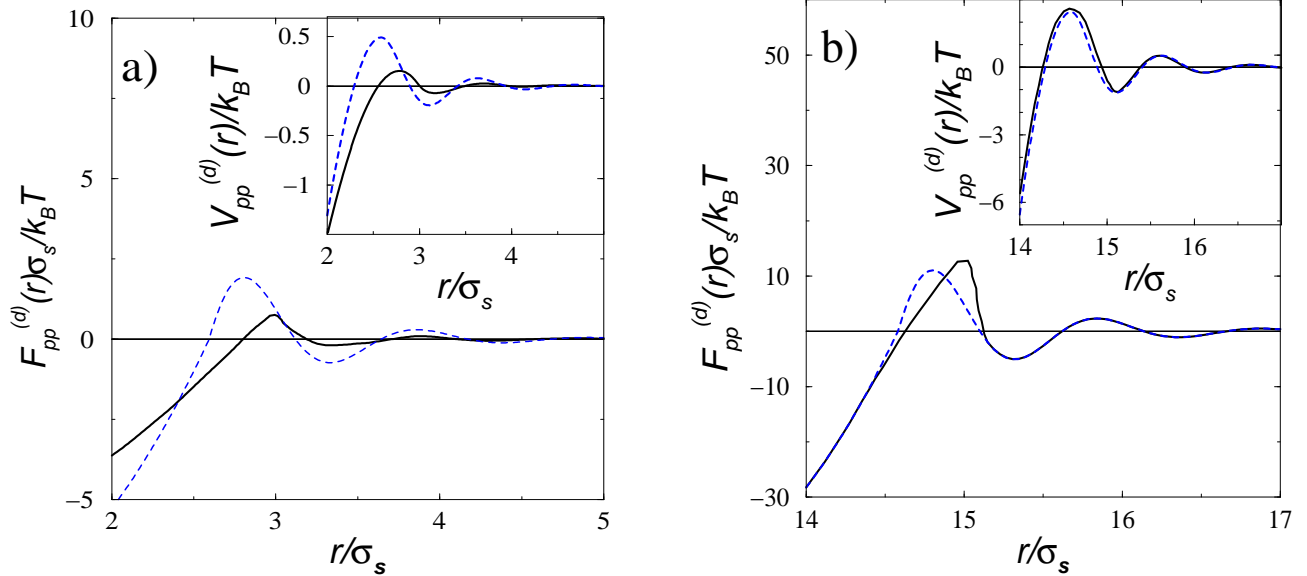


FIG. 2. Reduced distance-resolved depletion force $F(r)\sigma_s/k_B T$ versus reduced distance r/σ_s between two identical neutral spheres embedded into solvent bath of packing fraction $\phi_s = 0.3$: a) size asymmetry of $\sigma_p : \sigma_s = 2 : 1$; b) size asymmetry of $\sigma_p : \sigma_s = 14 : 1$. Solid line- our simulation results, dashed line- fitting formula of Ref.[38]. The inset shows the corresponding reduced depletion potentials $V_{pp}^{(d)}(r)/k_B T$.

simulation, the effective potential $V_{pp}^{(d)}(r)$ can be accessed by integrating the distance-resolved computer simulation results of the force

$$V_{pp}^{(d)}(r) = - \int_{-\infty}^r dr' F_{pp}^{(d)}(r') \quad (9)$$

Also the whole set of depletion pair potentials $V_{ij}^{(d)}(r)$ ($(ij) = (pp), (pc), (cc)$) which are the input of a typical SPM simulation are presented in Figure 3. The counterion-counterion interaction is dominated by the Coulomb repulsion also shown as a dashed line in Figure 3c. The bare Coulomb repulsion between the polyions is much larger than the polyion-polyion depletion potential and is not shown in Figure 3a. Finally, the polyion-counterion depletion interaction exhibits a deep attraction near contact of the order of $k_B T$ which is of similar order than the Coulomb attraction also shown as a dashed line on Figure 3b. This will have important consequences of counterion adsorption on the colloidal surface. This effect is induced by the granularity of the solvent and is absent in the PM.

V. RESULTS FOR THE SALT-FREE CASE

A. Nano-sized colloids

Although the amount of solvent which has to be simulated explicitly has been reduced drastically by the solvent-bath scheme, only colloidal sizes which are in the nano-domain can be addressed on present-day computers. We have performed extensive computer simulation in

this domain to check carefully the different approaches. We find that the SPM describes the full simulation data of the HSSM very well. Larger colloidal sizes are thus only accessible within the SPM and discussed in chapter V.B.

In our simulations, we fixed $T = 298^\circ K$ and $\epsilon = 81$ (water at room temperature) with $\sigma_s = 3\text{\AA}$, $\phi_s = 0.3$ such that ξ is about $3\sigma_s$. We varied the polyion charge and size and the counterion diameter σ_c . The width of the spherocylindrical cell h is $10\sigma_c$ such that typically $N_s = 25.000 - 30.000$ solvent hard spheres are simulated.

We have basically calculate two quantities: first, as a reference, we have calculated the spherically averaged counterion density profile $\rho_c(r)$ around a single polyion where r is the distance from the polyion center. The simulation was done in a cubic box of reduced length $L/2^{1/3}$ with periodic boundary conditions in order to reproduce the colloidal packing fraction ϕ_p . Second, our target quantity is the total force $F(r)$ acting onto a polyion for a given colloid-colloid separation r . This effective force $F(r)$ is the sum of four different contributions:

- i) the direct Coulomb repulsion as embodied in $V_{pp}(r)$ (note that all the periodic images contribute to the total force),
- ii) the counterion screening resulting from the averaged Coulomb force of counterions acting onto the polyions,
- iii) the counterion depletion term arising from the hard sphere part of $V_{pc}(r)$,
- iv) the solvent depletion force.

Explicit results for $F(r)$ are presented in Figure 4 where the solvent and the counterion diameter were chosen to be equal and the counterion were monovalent.

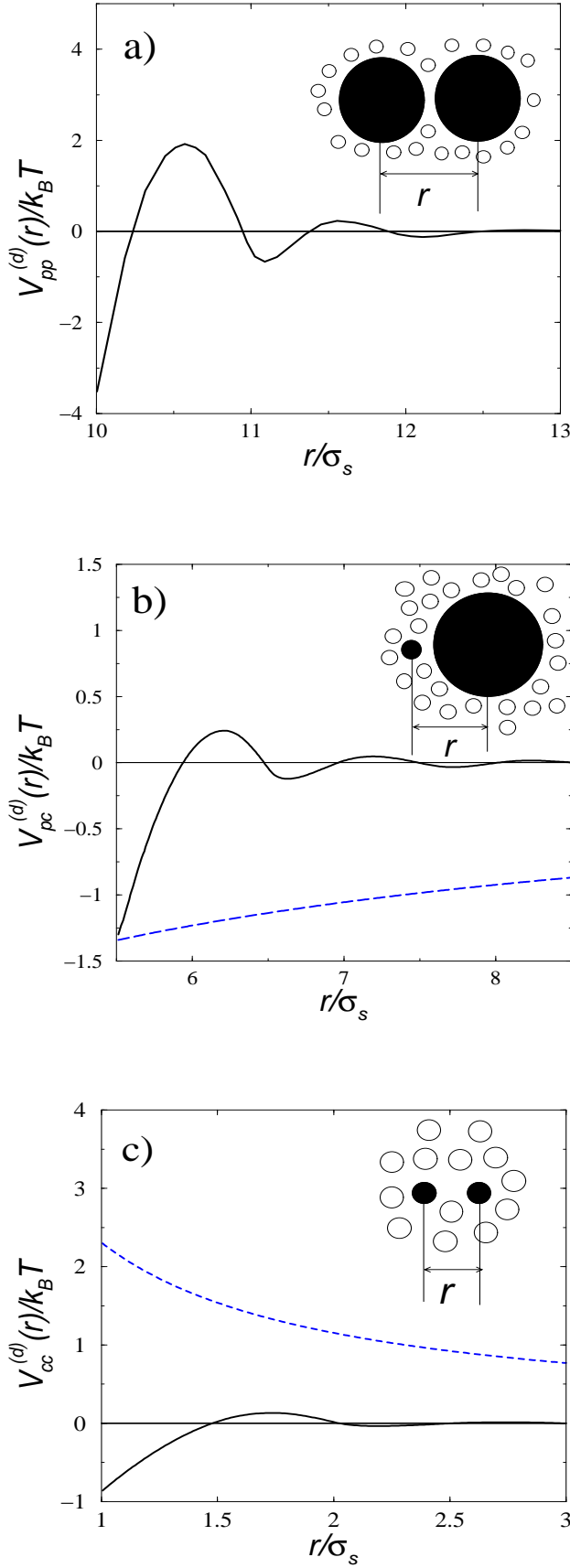


FIG. 3. Reduced depletion potentials $V_{ij}^{(d)}(r)/k_B T$ ($(ij) = (pp), (pc), (cc)$) versus reduced distance r/σ_s : a) polyion-polyion depletion with $\sigma_p/\sigma_s = 10$; b) polyion-counterion depletion with $\sigma_p : \sigma_c : \sigma_s = 10 : 1 : 1$; c) counterion-counterion depletion with $\sigma_c/\sigma_s = 1$. The solvent packing fraction is $\phi_s = 0.3$. The inset shows the situation. The dark spheres correspond to the pair of charged particles, the solvent are the hollow spheres. The x -axis starts for touching particles. For comparison we have also included the Coulomb interaction of the PM as dashed lines in b) and c) for $q_p = -32e, q_c = 1e$ and $\epsilon = 81$. Note that, the polyion-counterion Coulomb potential in plot 3b is reduced by a factor of $1/10$.

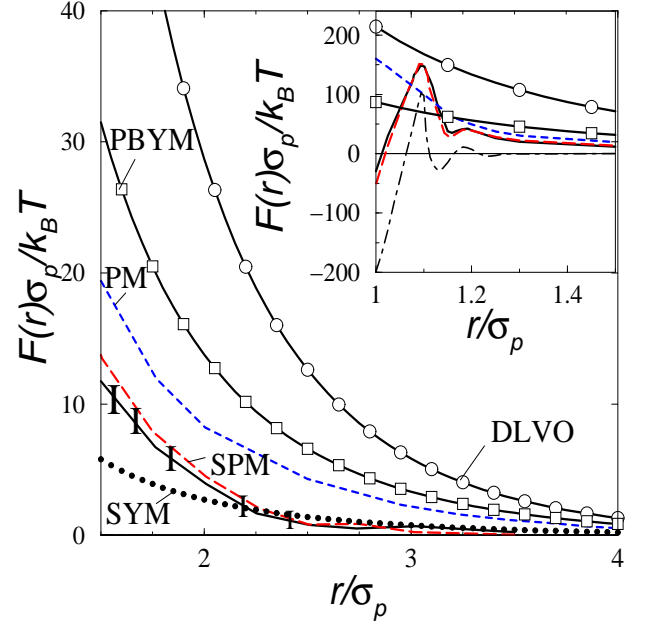


FIG. 4. Reduced distance-resolved force $F(r)\sigma_p/k_B T$ versus reduced distance r/σ_p . The inset shows the same for nearly touching polyions of molecular distances. The simulation parameters are: $q_c = 1e, q_p = -32e, \epsilon = 81, \sigma_p : \sigma_c : \sigma_s = 10 : 1 : 1, \phi_p = 5.8 \times 10^{-3}$. Solid line with error bars: -HSSM; long-dashed line: SPM; short-dashed line: PM; open circles: DLVO theory; open squares: PBYM theory; dotted line : SYM theory; dot-dashed line in inset: solvent depletion force (for comparison).

The force exhibits oscillations for molecular distances due to solvent and counterion layering and is repulsive for larger distances. The SPM yields surprising agreement with the HSSM describing even the molecular oscillations for nearly touching polyions, see the inset of Figure 4, while the PM overestimates the force considerably. This can be attributed to the fact that the SPM incorporates the additional counterion accumulation at the colloidal surface due to the hydration or solvent depletion. This can clearly be seen in the counterionic density profile around a polyion as shown in Figure 5 which piles up near the colloidal surface. While this accumula-

tion is quantitatively described by the SPM it is absent in the ordinary PM. The PBYM and DLVO theory lead to forces which strongly overestimate the HSSM data.

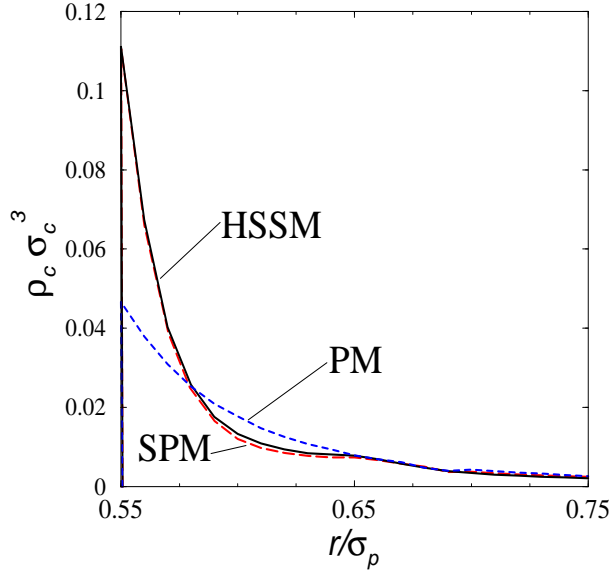


FIG. 5. Reduced counterion density profile $\rho_c \sigma_c^3$ around a single polyion versus reduced distance r/σ_p from the polyion center. The parameters and the line types are as in Figure 4.

We have further tested the frequently invoked “*superposition principle*” which approximates the total force as a sum of the PM and the depletion term. Its comparison to the full HSSM data is given in Figure 6a. The first maximum of the total force is semi-quantitatively reproduced but the superposition principle predicts a second maximum which is too sharp as compared to the HSSM data. This becomes even worse for a doubled counterion diameter of 6\AA where the superposition predicts a secondary maximum which is completely absent in the HSSM data, see Figure 6b. The physical reason for that is that the counterion layering coupled to the solvent degrees of freedom becomes relevant for these distances.

The forces for a doubled counterion diameter σ_c are presented in Figure 7. For small distances (except for touching), the PM yields larger forces as compared to Figure 4, as the counterion repulsion is stronger which reduces screening. In the HSSM and SPM, on the other hand, also the polyion-counterion depletion attraction is getting stronger, such that the total polyion screening is practically unaffected. Of course, the PBYM and DLVO theory yield results which are insensitive to the counterion diameter.

Furthermore we have investigated the case of stronger Coulomb coupling by considering divalent counterions. Explicit data are shown in Figure 8. There is overscreening of polyions resulting in a mutual attraction between like-charged polyions. We emphasize that it is the electrostatic term of the counterions that produces the attraction but not the counterion or solvent depletion term.

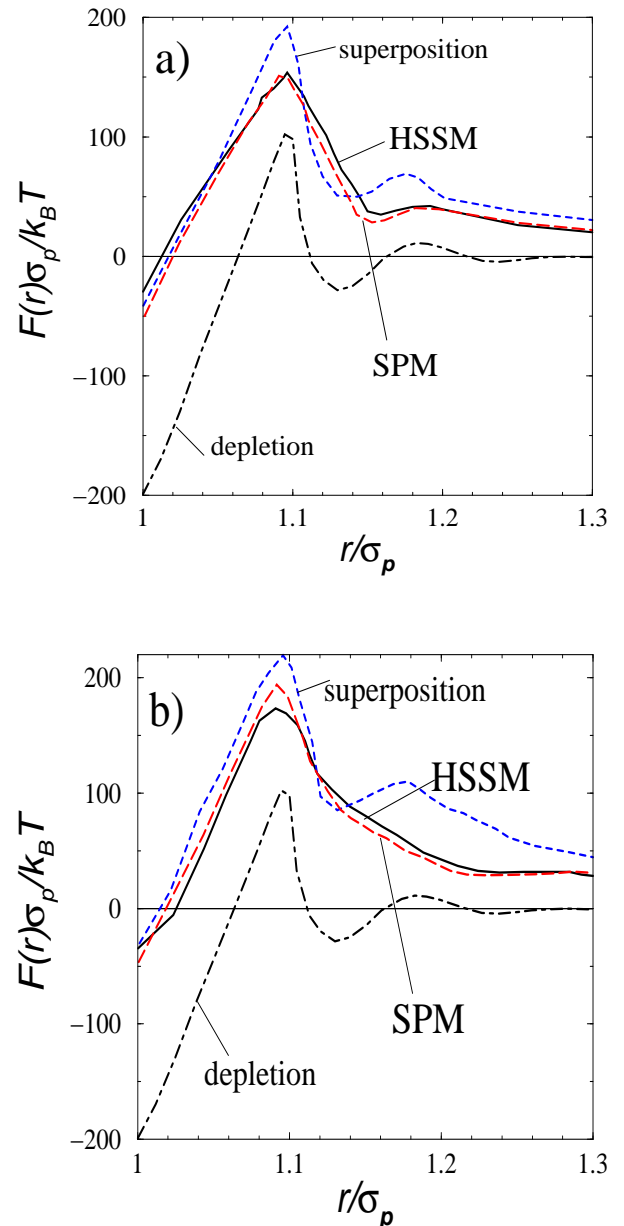


FIG. 6. Test of the superposition principle: reduced distance-resolved force $F(r)\sigma_p/k_B T$ versus reduced distance r/σ_p for two different counterion sizes: a) $\sigma_c = 3\text{\AA}$, b) $\sigma_c = 6\text{\AA}$. The force predicted by the superposition principle is the short-dashed line. The other parameters and notations are the same as in Figure 4.

Nearly every counterion is in the presence of the colloidal surfaces, as demonstrated by the counterionic density profile shown in Figure 9 where the piling-up of counterions near the colloidal surface is much stronger. The attractive force has a range of several polyion diameters. Again the SPM perfectly reproduces the forces. The PM (and also the PBYM and DLVO theory), on the other hand, yield repulsion. This demonstrates that a discrete solvent has a profound influence on the effective interactions.

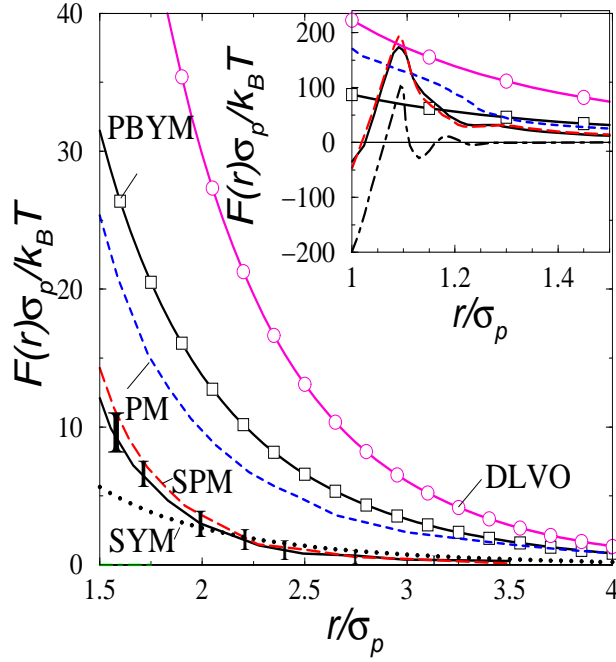


FIG. 7. Same as in Figure 4 but now for a double counterion diameter such $\sigma_p : \sigma_c : \sigma_s = 10 : 2 : 1$.

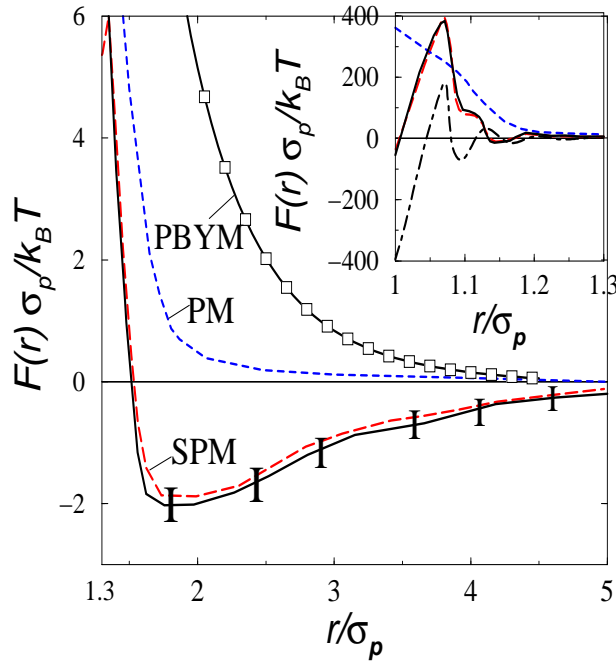


FIG. 8. Same as in Figure 7 but now for divalent counterions and $\sigma_p : \sigma_c : \sigma_s = 14 : 2 : 1$. The further parameters are $|q_p/q_c| = 32$ and $\phi_p = 5.8 \times 10^{-3}$.

We finally discuss the validity of the solvent-renormalized Yukawa model (SYM). Computer simulations have been performed for a single polyion in a spherical cell and the counterion boundary density was calculated. The boundary of the cell was not hard but coun-

terions leaving the cell were inserted at the opposite side of the cell. Again a smaller spherical solvent bath around the polyions with a width h was used, see Figure 10 for the set-up and a projected simulation snapshot. As Figures 4 and 7 show, the SYM is indeed a reasonable description of the forces for large distances. We also remark that the SPM and the HSSM yield the same counterion density at the boundary of the spherical cell needed as an input for the SYM which justifies the usage of the SPM to get the solvent-renormalized Yukawa parameters of the SYM.

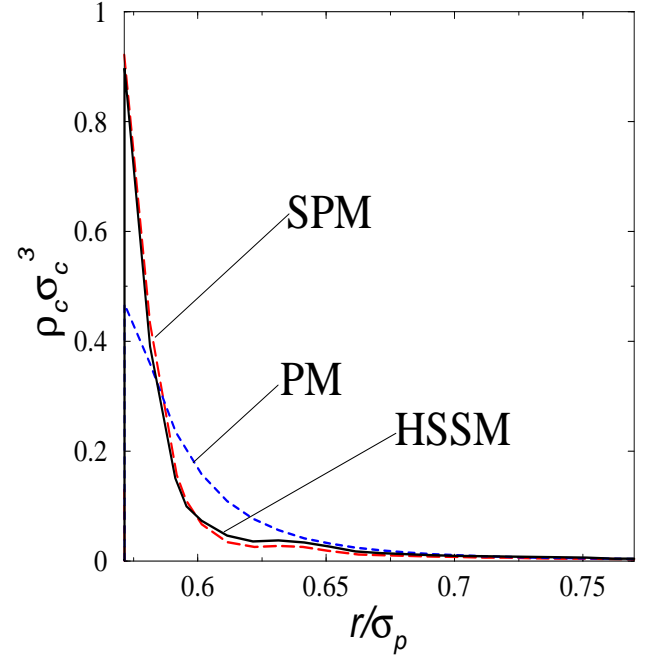


FIG. 9. Same as Figure 5 but now with the parameters of Figure 8.

The validity of the SYM only holds for the case of monovalent counterions where the remaining “free” counterions are responsible for the screened, repulsive force. For divalent counterions, no free counterions are left, and a linearized screening theory breaks down such that an attraction cannot be encapsulated by the SYM.

B. Mesoscopically-sized colloids

Our results for mesoscopically-sized colloids are based on SPM simulations as justified in the previous chapter. Distance-resolved colloidal forces $F(r)$ for monovalent counterions, a size asymmetry of $\sigma_p : \sigma_c : \sigma_s = 370 : 1 : 1$ or $370 : 2 : 1$, and a charge ratio of $q_p/q_c = 280$ are presented in Figure 11. These forces are repulsive but much smaller than that from PM simulations. Again, this is due to counterion accumulation near the colloidal surface as induced by the additional solvent depletion attraction. As the corresponding potential energy gain is

only few $k_B T$, this depletion attraction is different from chemisorption of counterions. The solvent-renormalized Yukawa model (SYM) leads to forces which are very similar to the SPM over the whole range of distances explored while the PM overestimates the forces.

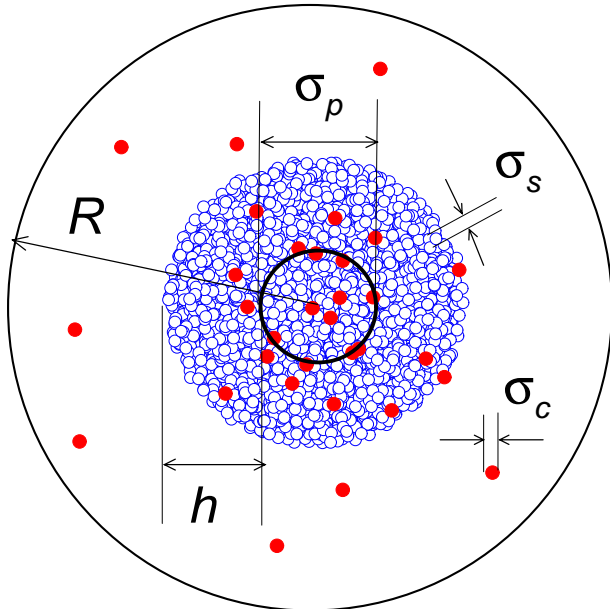


FIG. 10. View of the set-up and projected simulation snapshot for a single polyion in a spherical Wigner-Seitz-cell. The polyion is shown as dark open circle in the cell in a bath of solvent particles (small hollow spheres) contained in a spherical cell of width h . The counterions are shown as small dark spheres. R is cell radius.

The traditional meaning of the “bare” charge q_p in the PM is not the full polyion charge but a smaller charge which results from a polyion charge reduction by strongly adsorbed (or condensed) counterions. This picture can also be tested against our results. We first have calculated the average number of counterions in a molecular shell around the colloids of width ξ . If the polyion charge is reduced by this amount and the PM is used to predict the effective interaction, the resulting force still overestimates the HSSM data, see the open diamonds in Figure 11a. In order to fit these data satisfactorily, one has to assume an unphysically large width of 5ξ to get a charge reduction that reproduces the SPM data. Hence the PM cannot be justified even with a polyion charge reduction. The reason for that are the weak hydration forces which are quite different from chemisorption providing a strong counterion binding with an energy gain of hundreds or thousands of $k_B T$. Furthermore, an arbitrary splitting into a fraction of condensed counterions and “free” counterions described by DLVO, Poisson Boltzmann or any other local density functional theory is not possible: near the colloidal surface the electric double layer is highly correlated such that fixing a fraction of counterions gives a completely different picture. Only if the fraction of free counterions is determined within an

approach that includes all these correlations (as in the SYM), a linearized screening theory far away from the colloidal surfaces is justified.

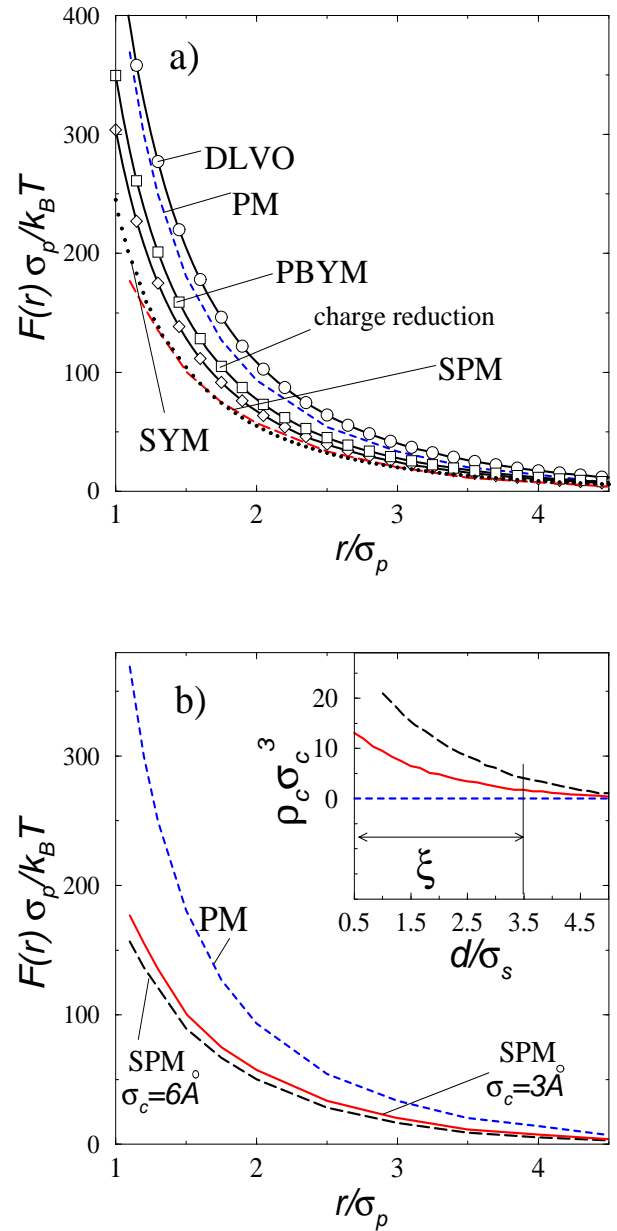


FIG. 11. Reduced distance-resolved force $F(r)\sigma_p/k_B T$ versus reduced distance r/σ_p for larger polyions, $\sigma_p : \sigma_c : \sigma_s = 370 : 1 : 1$, $|q_p/q_c| = 280$, $\phi_p = 2.3 \times 10^{-3}$, and monovalent counterions. a) Long-dashed line: SPM; short-dashed line: PM; open circles: DLVO theory; open squares: PBYM; open diamonds: PM with charge reduction, dotted line : SYM. b) Long-dashed line: SPM for a doubled counterion diameter $\sigma_c = 6\text{\AA}$; solid line: SPM for $\sigma_c = 3\text{\AA}$; dashed line: PM. The inset shows the corresponding reduced counterion density profile in the vicinity of a single polyion versus reduced distance d/σ_s , d being the distance from polyion surface.

This consideration casts some doubts to some recent theories where such a partitioning of counterions is an input, see e.g. Refs. [39,40]. Further SPM results for a doubled counterion diameter are presented in Figure 11b. As the counterion depletion force is getting stronger for a large counterion, the force is getting smaller, compare the full and dashed line in Figure 11b. The PM (short-dashed line in Figure 11b), on the other hand, is practically insensitive to a change of the counterion diameter except very close to the colloidal surfaces. This picture gains further support from the counterionic density profiles around a single polyion shown in the inset of Figure 11b for distances very close to the colloidal surface. A layer of condensed but still mobile counterions close to the surfaces is present in the SPM which is absent in the PM. The larger the counterion diameter the more counterions are in this layers as the depletion is getting stronger.

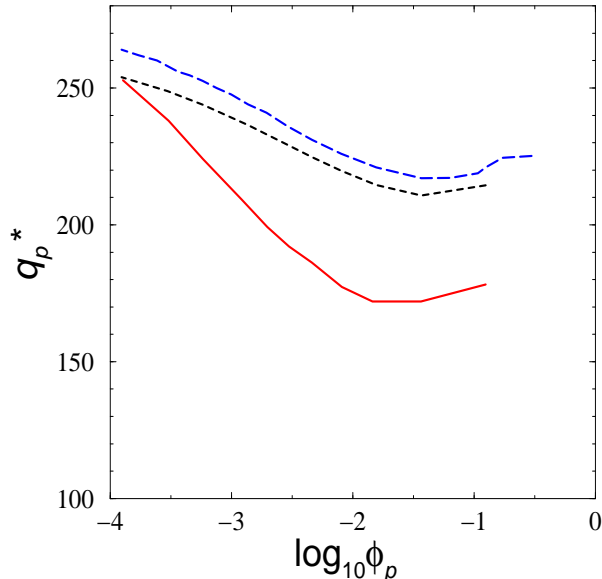


FIG. 12. Renormalized charge q_p^* versus decadic logarithm $\log_{10} \phi_p$ of the polyion fraction as obtained within in spherical cell containing a single polyion. The parameters are the same as in Figure 11. Solid line: SPM; long dashed line: PBYM; dashed line: PBYM for a fixed bare charge of $q_p = 269e$.

We finally discuss the solvent-renormalized charge q_p^* as a function of the colloid volume fraction ϕ_c for fixed bare charge q_p and compare with the prediction of the traditional charge renormalization approach within in Poisson Boltzmann cell theory (PBYM) [10]. Simulation data for q_p^* based on the SPM in a spherical cell are shown on the full line in Figure 12. The renormalized charge is smaller than the bare charge and behaves non-monotonic with the particle density. The non-monotonicity is stable with respect to added salt and is related to a non-monotonic counterion density at the cell boundary as a function of density. It can be understood as follows: For extremely high packing fractions the spherical cell acces-

sible for the counterions is a very thin shell across which the polyion-counterion attraction varies slowly. Due to the rapidly decreasing volume accessible for the counterions, the boundary counterion density becomes larger for increasing ϕ_p , see the volume fraction correction in Refs. [41,42]. On the other hand, for very small ϕ_p , entropy of counterions will force them to cover the whole accessible space. The counterion density at the cell boundary will increase for decreasing ϕ_p getting close to the average density in the limit $\phi_p \rightarrow 0$. We remark, however, that the non-monotonicity occurs at high polyion packing fractions of order $\phi_p \approx 0.05 - 0.2$ where the approximation of a spherical cell becomes questionable.

The PBYM for a fixed bare charge leads to larger values (long-dashed line in Figure 12) which still correctly describe the trend and the non-monotonicity. If the SPM data for the smallest colloid concentration are taken as a benchmark, a bare charge of $q_p = 269e$ is necessary to reproduce the same renormalized charge within the Poisson-Boltzmann theory. This procedure is in strong analogy with interpreting an experiment where the charge is a fit parameter to describe the structural data. Starting from this bare charge and changing the colloidal density, the PBYM predicts a similar trend for the renormalized charge (short-dashed line in Figure 12) but the actual numbers are different. This is consistent with experiments on strongly deionized colloidal samples which were successfully interpreted using a Poisson-Boltzmann renormalized colloidal charge [28,30,29].

VI. EFFECTS OF ADDED SALT

Within the HSSM, the salt ions enter as charged hard spheres. For simplicity, we have considered a situation where the salt ions are monovalent and have the same diameter as the counterions and the solvent. Results for the effective interactions for a case with added salt are presented in Figure 13. As expected, the salt ions provide an additional screening such that the forces are less repulsive than in the salt-free case (compare with Figure 4). The SPM reproduces the full HSSM data for intermediate distances but there are deviations for molecular distances. This is in contrast to the salt-free case where good agreement between the SPM and the HSSM was found even for small distances. The physical reason for this is that the pair potential decomposition which is the basic approximation of the SPM breaks down for nearly touching polyions as important configurations are paired microions squeezed between the polyions. This is a manifest many-body situation beyond the pair level. Still for two well-separated polyions or a single polyion, the SPM and the HSSM yield similar results for the counterion density field or the colloidal forces.

As in the salt-free case, we have tested the PBYM. The solvent-renormalized charge q_p^* as obtained from the SPM is plotted as a solid line in Figure 14 versus salt

concentration. It decreases for increasing salt concentration. The PBYM for the same bare charge of $q_p = 280e$ yields the same trend as obtained in earlier investigations [43], see the long-dashed line in Figure 14. If scaled by

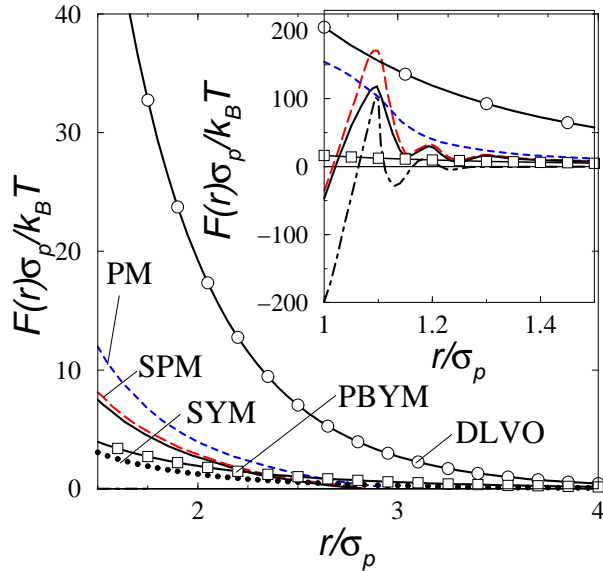


FIG. 13. Same as in Figure 4 but now for added monovalent salt, $c_s = 0.022\text{Mol/l}$.

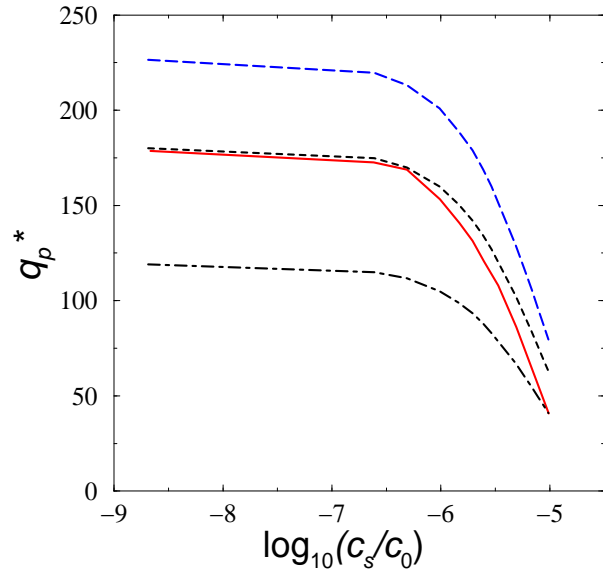


FIG. 14. Renormalized charge q_p^* versus decadic logarithm $\log_{10}(c_s/c_0)$ of the salt concentration where $c_0 = 1\text{Mol/l}$ is a reference salt concentration. The parameters are the same as in Figure 11 but now $\phi_p = 8 \times 10^{-3}$ and $\sigma_c = 3\text{\AA}$. Solid line: SPM; long dashed line: PBYM; dashed line: PBYM for a fixed bare charge of $q_p = 210e$; dot-dashed line: PBYM for a fixed bare charge of $q_p = 130e$.

using the SPM data for the salt-free case as a benchmark (short-dashed line in Figure 14), the trend obtained

in the PBYM is almost the same as that in the SPM. This explains the success of fitting experimental data [44,28,30,29] by using the PBYM for real colloidal samples which typically contain a lot of added salt. If the SPM data for a high concentration of added salt is used as benchmark point, the PBYM predicts much smaller renormalized charge upon deionization (dot-dashed line in Figure 14).

VII. COMMENTS ON OTHER MECHANISMS FOR POLYION-POLYION ATTRACTION

We finally comment on two other physical mechanism for mutual attraction between like-charge colloids. The first is the counterion depletion mechanism which was found within the PM in salt-free colloidal suspensions with strong Coulomb coupling (as realized by a small dielectric constant) [5]. We have redone the simulation using the same parameters as in Ref. [5] but now with added salt. The depletion attraction is reduced but still present, see Figure 15. As put forward in Ref. [5], the range of the attraction is comparable to

$$a = \sqrt{q_c/q_p} \sqrt{4\pi/\sqrt{3}\sigma_p} \quad (10)$$

which is a typical counterion distance corresponding to the spacing of a triangular lattice on the spherical colloidal surface. This length is also included in Figure 15.

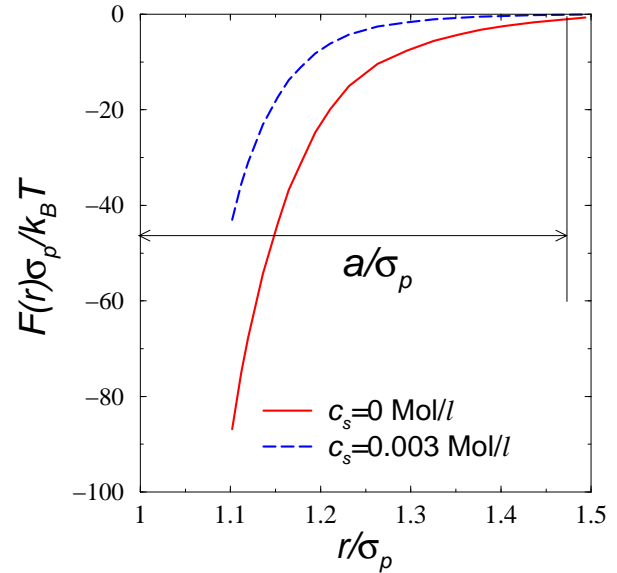


FIG. 15. Reduced distance-resolved force $F(r)\sigma_p/k_B T$ versus reduced distance r/σ_p . The counterions are divalent and the size asymmetry is $\sigma_p : \sigma_c : \sigma_s = 33 : 1 : 1$. The further parameters are $|q_p/q_c| = 16$, $\epsilon = 5$ and $\phi_p = 1.6 \times 10^{-2}$. Solid line: PM without salt; long-dashed line: PM with monovalent salt at concentration $c_s = 0.003\text{Mol/l}$. The range $a/\sigma_p = 0.476$ of the depletion attraction is also indicated.

Unfortunately, the polyion radius used in Ref. [5] is too large to allow for a reasonable number of solvent particles in the solvent bath. Therefore we have slightly reduced the polyion size such that the PM yields the same counterion depletion-mediated attraction. Results based on the HSSM and PM are collected in Figure 16. As can be deduced from this figure, the depletion-mediated attraction is stable with respect to an explicitly added solvent. It is further stable but reduced with respect to added salt. However, an added solvent reduces the attraction a bit. The physical reason for that is that the solvent will prefer to stay in the counterion-free space near the colloidal surfaces such that the solvent depletion cancels part of the counterion depletion force.

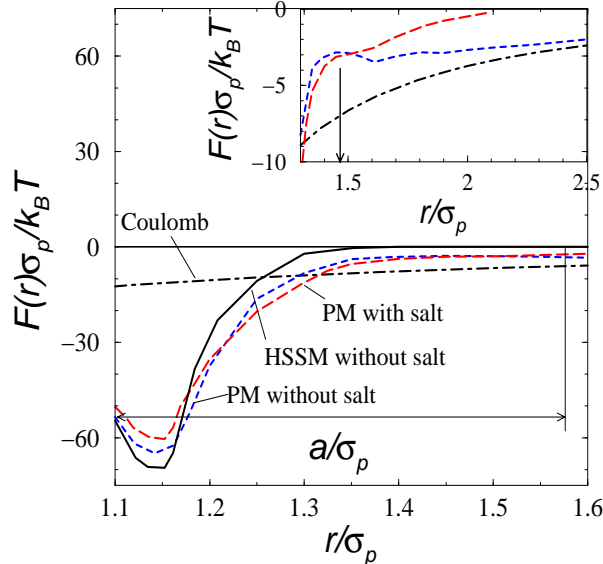


FIG. 16. Reduced distance-resolved force $F(r)\sigma_p/k_B T$ versus reduced distance r/σ_p for divalent counterions and $\sigma_p : \sigma_c : \sigma_s = 10 : 1 : 1$. The further parameters are $|q_p/q_c| = 16$, $\epsilon = 20$ and $\phi_p = 5.8 \times 10^{-3}$. Solid line: HSSM without salt; long dashed line- PM result with added monovalent salt at concentration $c_s = 2.74 \times 10^{-4}$ Mol/l; dashed line: PM without salt; dot-dashed line: pure electrostatic interaction between a pair of $+2e$ and $-2e$ ions. The depletion range $a/\sigma_p=0.476$ is also shown. The long range tails of the forces are compared in the inset. The arrow there indicates the range a .

Second, we comment on the mechanism of metastable oppositely-ionized colloids leading to long-ranged Coulomb attraction as found in recent salt-free PM simulations by Messina et al [7]. We have confirmed and reproduced this effect in our simulations for the parameters of Figure 16. We found, however, that the opposite ionization of the colloids will be immediately suppressed if salt is added. In Figure 16, it is shown that for large distances the salt-free PM data are close to the long-ranged Coulomb force for an ionization degree by one counterion (compare the dot-dashed and the short-dashed line in the inset of Figure 16). Once

salt is added, however, the additional microscopic ions will be attracted directly towards the ionized polyions and the long-ranged Coulomb attraction disappears (see the long-dashed line in the inset of Figure 16). Hence, the mechanism of attraction due to metastable ionized states is not stable with respect to added salt. We also remark that metastable ionized states will disappear for separations shorter than the characteristic depletion zone length a . For such close configurations, the mutual attractive Coulomb correlations in the counterion cloud around both polyions will lead to a symmetric shearing of counterions by the two neighboring polyions. For such small separations, counterion depletion is responsible for the attraction. As a function of distance, the total force is nonmonotonic. For small distances it is dominated by counterion depletion which decays off rapidly on the scale a , while for larger distances the electrostatic resulting from the metastable oppositely-ionized colloids leads to a long-ranged attraction.

VIII. CONCLUSIONS

In conclusion, based on simulations of a model which contains the granularity of the solvent explicitly, we have shown that hydration forces profoundly influence the colloidal interaction. For divalent counterions, there is solvent-induced attraction which is not contained in the traditional primitive model but can be captured within a solvent-averaged primitive model (SPM). For monovalent counterions, the forces can be described by a solvent-induced *charge renormalization*. This picture is in agreement with experiments on strongly deionized samples where a Yukawa picture can be employed provided the colloidal charge is renormalized towards a value smaller than the bare charge [45]. The trends of the renormalized charge upon increasing the salt concentration is similar in the Poisson-Boltzmann cell model and the SPM which explains why the experimental data could be well-described by using a Yukawa interaction with a Poisson-Boltzmann-renormalized charge [28,30,29]. Still, quantitatively, there are differences between the renormalized charges of the Poisson-Boltzmann cell model and the SPM.

Future research should focus on the role of the permanent dipole moment in a polar solvent as modelled by dipolar hard spheres [55,56] or a Stockmayer liquid [57]. Also more work has to be done to explore the role of charge regulation and chemisorption of counterions near the colloidal surfaces. Furthermore the dielectric discontinuity at the colloidal surfaces resulting in image charge effects has to be explored in more detail. For all these circumstances the concept of a renormalized polyion charge resulting in a Yukawa picture should be possible provided there are free counterions left which dominate the effective repulsion between the colloids.

We finally point out further possible applications of

our simulation technique: If used without the confining solvent-bath shell, our approach starts “ab initio” and even employs the correct microscopic (molecular) dynamics of the solvent. Therefore, it could also be used to address dynamical questions in equilibrium and non-equilibrium. Important examples concern the motion of poly- and counterions under the influence of an external electric field including effects as the electrophoretic mobility [46–49], ion migration [50], electro-kinetic properties [51] and electrolyte friction [52,53]. Our approach produces both diffusive motion and hydrodynamic interactions mediated by the solvent as an output. Of course, one will not be able to simulate large time scale separations between the Brownian and the structural relaxation time [54] but one should try to start with moderate time scale separations in order to test the approximative theories of electrophoresis.

We thank R. Roth, M. Schmidt and T. Palberg for helpful remarks and the DFG for financial support.

-
- [1] “Structure and Dynamics of Strongly Interacting Colloids and Supramolecular Aggregates in Solution” edited by S.-H. Chen, J. S. Huang, P. Tartaglia, NATO ASI Series, Vol. 369, Kluwer Academic Publishers, Dordrecht, 1992.
- [2] J. P. Hansen, H. Löwen, *Ann. Rev. Phys. Chemistry*, October 2000, in press.
- [3] B. Hribar, V. Vlachy, *J. Chem. Phys. B* **101**, 3457 (1997); *Biophysical Journal* **78**, 694 (2000).
- [4] N. Gronbech-Jensen, K. M. Beardmore, P. Pincus, *Physica A* **261**, 74 (1998).
- [5] E. Allahyarov, I. D’Amico, H. Löwen, *Phys. Rev. Lett.* **81**, 1334 (1998).
- [6] P. Linse, V. Lobaskin, *Phys. Rev. Lett.* **83**, 4208 (1999); *J. Chem. Phys.* **112**, 3917 (2000).
- [7] R. Messina, C. Holm, K. Kremer, *Phys. Rev. Lett.* **85**, 872 (2000).
- [8] H. Löwen, J. P. Hansen, P. A. Madden, *J. Chem. Phys.* **98**, 3275 (1993).
- [9] B. V. Derjaguin, L. D. Landau, *Acta Physicochim. USSR* **14**, 633 (1941); E. J. W. Verwey and J. T. G. Overbeek, “Theory of the Stability of Lyophobic Colloids” (Elsevier, Amsterdam, 1948).
- [10] S. Alexander, P. M. Chaikin, P. Grant, G. J. Morales, P. Pincus, D. Hone, *J. Chem. Phys.* **80**, 5776 (1984).
- [11] D. E. Smith, L. X. Dang, *J. Chem. Phys.* **100**, 3757 (1994).
- [12] M. Kinoshita, S. Iba, M. Harada, *J. Chem. Phys.* **105**, 2487 (1996).
- [13] F. Otto, G. N. Patey, *Phys. Rev. E* **60**, 4416 (1999); *J. Chem. Phys.* **112**, 8939 (2000).
- [14] S. Marcelja, *Colloids and Surfaces A* **129-130**, 321 (1997).
- [15] V. Kralj-Iglic, A. Iglic, *J. Physique II (France)* **6**, 477 (1996); J. Borukhov, D. Andelman, H. Orland, *Phys. Rev. Lett.* **79**, 435 (1997); Y. Burak, D. Andelman, to be published, E. Trizac, J.-L. Raimbault, *Phys. Rev. E* **60**, 6530 (1999).
- [16] Z. Tang, L. E. Scriven, H. T. Davis, *J. Chem. Phys.* **100**, 4527 (1994); L. J. D. Frink, F. van Swol, *J. Chem. Phys.* **105**, 2884 (1996); T. Biben, J. P. Hansen, Y. Rosenfeld, *Phys. Rev. E* **57**, R3727 (1998) C. N. Patra, *J. Chem. Phys.* **111**, 9832 (1999); D. Henderson, P. Bryk, S. Sokolowski, D. T. Wasan, *Phys. Rev. E* **61**, 3896 (2000).
- [17] See e.g.: D. Boda, D. Henderson, *J. Chem. Phys.* **112**, 8934 (2000).
- [18] J. Rescic, V. Vlachy, L. B. Bhuiyan, C. W. Outhwaite, *J. Chem. Phys.* **107**, 3611 (1997).
- [19] S. Marcelja, *Langmuir* **16**, 6081 (2000).
- [20] W. G. McMillan, J. E. Mayer, *J. Chem. Phys.* **13**, 276 (1945).
- [21] E. Allahyarov, H. Löwen, to be published.
- [22] T. Biben, J. P. Hansen, *Europhys. Lett.* **12**, 347 (1990).
- [23] M. Dijkstra, R. van Roij, R. Evans, *Phys. Rev. Lett.* **81**, 2268 (1998); *Phys. Rev. E* **59**, 5744 (1999).
- [24] B. Götzelmann, R. Roth, S. Dietrich, M. Dijkstra, R. Evans, *Europhys. Lett.* **47**, 398 (1999).
- [25] R. Roth, B. Götzelmann, S. Dietrich, *Phys. Rev. Lett.* **83**, 448 (1999).
- [26] R. Dickman, P. Attard, V. Simonian, *J. Chem. Phys.* **107**, 205 (1997).
- [27] M. Dijkstra, R. van Roij, R. Evans, *Phys. Rev. Lett.* **82**, 117 (1999).
- [28] W. Härtl, H. Versmold, *J. Chem. Phys.* **88**, 7157 (1988).
- [29] F. Bitzer, T. Palberg, H. Löwen, R. Simon, P. Leiderer, *Phys. Rev. E* **50**, 2821 (1994).
- [30] T. Palberg, W. Mönch, F. Bitzer, R. Piazza, T. Bellini, *Phys. Rev. Lett.* **74**, 4555 (1995).
- [31] J. C. Crocker, D. G. Grier, *Phys. Rev. Lett.* **73**, 352 (1994); G. M. Kepler, S. Fraden, *Phys. Rev. Lett.* **73**, 356 (1994); D. G. Grier, *Nature (London)* **393**, 621 (1998).
- [32] I. D’Amico, H. Löwen, *Physica A* **237**, 25 (1997).
- [33] E. Allahyarov, H. Löwen, S. Trigger, *Phys. Rev. E* **57**, 5818 (1998).
- [34] T. Biben, P. Bladon, D. Frenkel, *J. Phys. Condensed Matter* **8**, 10799 (1996).
- [35] D. Rudhardt, C. Bechinger, P. Leiderer, *Phys. Rev. Lett.* **81**, 1330 (1998).
- [36] J. C. Crocker, J. A. Matteo, A. D. Dinsmore, A. G. Yodh, *Phys. Rev. Lett.* **82**, 4352 (1999).
- [37] C. Bechinger, D. Rudhardt, P. Leiderer, R. Roth, S. Dietrich, *Phys. Rev. Lett.* **83**, 3960 (1999).
- [38] R. Roth, R. Evans, to be published.
- [39] M. N. Tamashiro, Y. Levin, M. C. Barbosa, *Physica A* **258**, 341 (1998).
- [40] V. I. Perel, B. I. Shklovskii, *Physica A* **274**, 446 (1999).
- [41] W. B. Russel, D. W. Benzing, *J. Colloid Interface Science* **83**, 163 (1981).
- [42] A. R. Denton, H. Löwen, *Phys. Rev. Lett.* **81**, 469 (1998).
- [43] M. J. Stevens, M. L. Falk, M. O. Robbins, *J. Chem. Phys.* **104**, 5209 (1996).
- [44] S. Bucci, S. Fagotti, V. Dergiorio, R. Piazza, *Langmuir* **7**, 824 (1991).
- [45] T. Gisler, S. F. Schulz, M. Borkovec, H. Sticher, P.

- Schurtenberger, B. D'Aguanno, R. Klein, *J. Chem. Phys.* **101**, 9924 (1994).
- [46] M. Evers, N. Garbow, D. Hessinger, T. Palberg, *Phys. Rev. E* **57**, 6774 (1998).
- [47] A. K. Gaigalas, S. Woo, J. B. Hubbard, *J. Colloid Interface Science* **136**, 213 (1990).
- [48] C. S. Mangelsdorf, L. R. White, *J. Chem. Soc. Faraday Trans.* **88**, 3567 (1992).
- [49] H. Ohshima, *J. Colloid Interface Science* **179**, 431 (1996); **188**, 481 (1997).
- [50] M. Wojcik, *Chem. Phys. Lett.* **260**, 287 (1996).
- [51] M. Deggelmann, T. Palberg, M. Hagenbüchle, E. E. Maier, R. Krause, C. Graf, R. Weber, *J. Colloid Interface Science* **143**, 318 (1991).
- [52] J. M. Schurr, *Chem. Phys.* **45**, 119 (1980).
- [53] G. Cruz de Leon, M. Medina-Noyola, O. Alarcon-Waess, H. Ruiz-Estrada, *Chem. Phys. Letters* **207**, 294 (1993); J. M. Mendez-Alcaraz, O. Alarcon-Waess, *Physica A* **268**, 75 (1999).
- [54] P. N. Pusey, in "Liquids, Freezing and the Glass Transition", edited by J. P. Hansen, D. Levesque and J. Zinn-Justin (North Holland, Amsterdam, 1991).
- [55] F. Lado, *J. Chem. Phys.* **106**, 4707 (1997).
- [56] J. J. Weis, *Mol. Phys.* **93**, 361 (1998).
- [57] B. Groh, S. Dietrich, *Phys. Rev. Lett.* **72**, 2422 (1994); **74**, 2617 (1995).